



HAL
open science

Registration of Arbitrary Multi-view 3D Acquisitions

Camille Chane Simon, Rainer Schutze, Frank Boochs, Franck Marzani

► **To cite this version:**

Camille Chane Simon, Rainer Schutze, Frank Boochs, Franck Marzani. Registration of Arbitrary Multi-view 3D Acquisitions. *Computers in Industry*, 2013, 64 (9), pp.1082-1089. 10.1016/j.compind.2013.03.017 . hal-00931793

HAL Id: hal-00931793

<https://hal.science/hal-00931793>

Submitted on 15 Jan 2014

HAL is a multi-disciplinary open access archive for the deposit and dissemination of scientific research documents, whether they are published or not. The documents may come from teaching and research institutions in France or abroad, or from public or private research centers.

L'archive ouverte pluridisciplinaire **HAL**, est destinée au dépôt et à la diffusion de documents scientifiques de niveau recherche, publiés ou non, émanant des établissements d'enseignement et de recherche français ou étrangers, des laboratoires publics ou privés.

Fusion of Arbitrary Multi-view 3D Acquisitions

Camille Simon Chane^{a,b}, Rainer Schütze^b, Frank Boochs^b, Franck S. Marzani^a

^a*le2i, Université de Bourgogne, B.P. 47870, 21078 Dijon, France*

^b*i3mainz, Fachhochschule Mainz, Lucy Hillebrand Straße 2, 55128 Mainz, Germany*

Abstract

Registration of 3D meshes of smooth surfaces is performed by tracking the acquisition system. The tracking is performed using photogrammetric techniques. Careful calibration of all objects in play enable a registration accuracy of *******. Targets are used to assess the precision of the registration, but the method does not rely on the use of targets and can be used for the registration of featureless surfaces.

Keywords: 3D imaging, close-range photogrammetry, 3D registration, multi-view registration

Contents

1	Introduction	1
2	Materials and Methods	2
2.1	Principle	2
2.2	Materials	3
2.3	Calibrations	3
2.4	Data processing	6
3	Results and Discussion	7
3.1	Individual calibrations	7
3.2	Tracking the frame	7
3.3	Registration	9
4	Conclusion and Perspectives	9

Email addresses: camille.simon@u-bourgogne.fr (Camille Simon Chane),
rainer.schuetze@geoinform.fh-mainz.de (Rainer Schütze),
frank.boochs@geoinform.fh-mainz.de (Frank Boochs), franck.marzani@u-bourgogne.fr
(Franck S. Marzani)

1. Introduction

3D imaging is increasingly used for surface inspection. Creating 3D models with contact-less imaging sensors is a greatly useful. However, there are natural trade-offs between the field of view of these devices and their resolution. To scan large objects with a high resolution, multiple acquisitions with complementary fields of view are necessary. These views must then be stitched together to create a complete 3D model. This is the problem of high-accuracy multi-view registration.

In the case of spatially-structured objects, multi-view registration is most often based on the ICP algorithm [1] or one of its variations [2]. This method does not perform well for smooth surfaces and requires a 30% to 40% overlap between successive views. On the other hand, basing the registration on feature points requires adequate salient points for each pair of datasets. Targets can be added to the surface if there are no natural salient features, if these features are not well-resolved or if they are insufficient in number. However, it can be tedious and time-consuming to place and remove targets from the multiple objects that we want to digitize. Furthermore, there is always the possibility that a target covers a defect that we want to detect. Also, there may be cases in which we fear damaging the surface with the targets.

Instead of relying on the object data, 3D registration can be based on the known position and orientation of the acquisition system. If a robot is used to control the acquisition system, its' position and orientation is readily available. But the attained accuracy of 1 mm in untaught mode is not sufficient to base the registration solely on this data. Optical techniques such as photogrammetry can be used to increase robot positioning accuracy via on-line calibration. Two setups are possible: either a camera is fixed to the robot and observes the scene which has been covered with targets [3, 4] or the robot is itself covered with targets and observed by a number of fixed cameras [5, 6]. This second setup is the best suited to be adapted to our task. We can measure the precise position and orientation of the acquisition system in a coordinate system defined by set of fixed cameras which observe the acquisition system the camera by fixing targets to it, instead of on the object under study. Our goal is to register 3D datasets with a precision better than half the acquisition system resolution.

2. Materials and Methods

2.1. Principle

Figure 1 illustrates the principle of our technique: a set of photogrammetric cameras observe an acquisition system while it digitizes a surface. A target-frame is fixed to the acquisition system to enable the precise tracking of its' position and orientation during the measurements.

The scope of this experiment is to show that this setup can be used to track a 3D acquisition system and to register the individual 3D acquisitions. The object

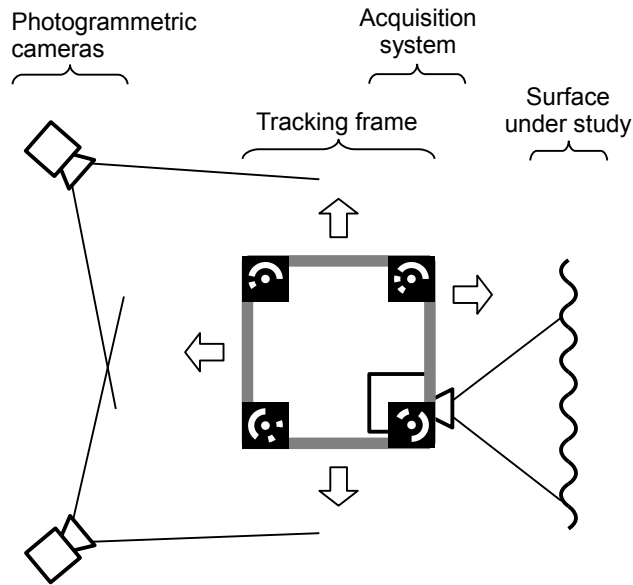


Figure 1: Overview of tracking configuration

42 under study is a car door which has been covered with un-coded photogram-
 43 metric targets. These targets are not used for the tracking and registration but
 44 they enable us to measure the accuracy of our registration procedure.

45 *2.2. Materials*

46 All 3D digitizations were performed using a commercial fringe projection
 47 digitization system by Gom, the Atos III. The system can be built in different
 48 field-of-view/ accuracy setups. For this study we use a $500 \text{ mm} \times 500 \text{ mm}$ field
 49 of view, yielding an accuracy of 0.24 mm . In this configuration the measuring
 50 distance between the Gom Atos III and the surface under study must be 760 mm .
 51 This entails that our registration accuracy goal of half the acquisition resolution
 52 is 0.12 mm spatially and 0.158 mrad .

53 The characteristics of the materials used for the tracking procedure were
 54 optimized through several simulations, some of which are described in [7]. The
 55 four tracking cameras are 5Mpx AVT Stingray and are used in conjunction
 56 with 8mm Pentax lens. The tracking frame is an aluminum cube of edge length
 57 500 mm and covered with 78 targets (see figure 2). A hexagonal headplate is
 58 attached to the bottom of the frame so that it can be fixed to a tripod. A
 59 hexagonal plate holder inside the cube on the bottom face is used to fix the
 60 acquisition system to the frame. An additional camera, a Nikon D300, is used
 61 for certain calibration procedures.

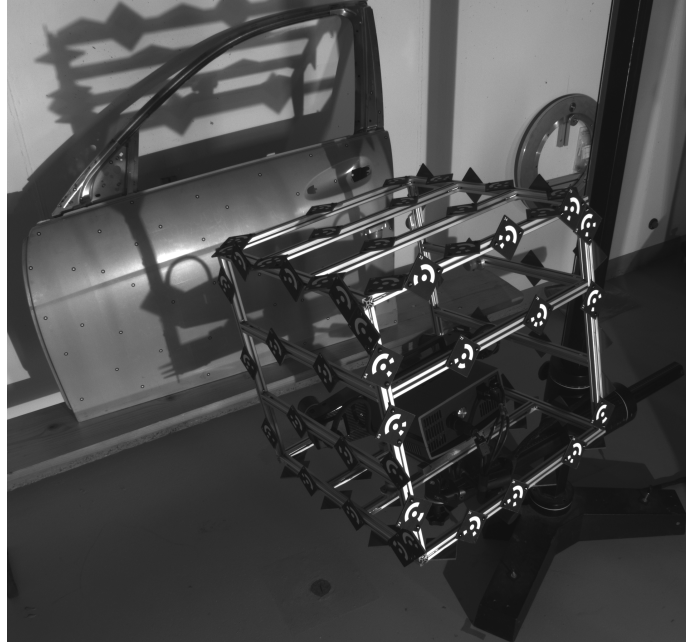


Figure 2: Tracking cube covered with 78 targets with the acquisition system fixed inside the cube. The car door is visible in the background.

62 *2.3. Calibrations*

63 To ensure a precise tracking, all optics and objects in play must be carefully
 64 calibrated. We thus introduce the following coordinate systems, linked to the
 65 materials in use (illustrated figure 3):

- 66 • $C_S, (O_S, \vec{x}_S, \vec{y}_S, \vec{z}_S)$ is the coordinate system linked to the acquisition sys-
 67 tem.
- 68 • $C_F, (O_F, \vec{x}_F, \vec{y}_F, \vec{z}_F)$ is the coordinate system linked to the tracking frame.
- 69 • $C_{C_i}, (O_{C_i}, \vec{x}_{C_i}, \vec{y}_{C_i}, \vec{z}_{C_i})$ are the coordinate systems linked to the each
 70 tracking camera. O_{C_i} is the optical center of the camera, $(\vec{x}_{C_i}, \vec{y}_{C_i})$ define
 71 the image plane, \vec{z}_{C_i} is collinear to the optical axis.
- 72 • $C_0, (O_0, \vec{x}_0, \vec{y}_0, \vec{z}_0)$ is the world coordinate system.

73 We now describe the necessary calibrations and how they are performed.
 74 The following notations will be used throughout this section: $A|_{C_U}$ are the
 75 homogeneous coordinates $(x_A, y_A, z_A, 1)$ of point A in coordinate system C_U .
 76 We define T_{C_U, C_V} the transformation matrix between two coordinate system
 77 C_U and C_V such that $T_{C_U, C_V} \cdot A|_{C_V} = A|_{C_U}$.

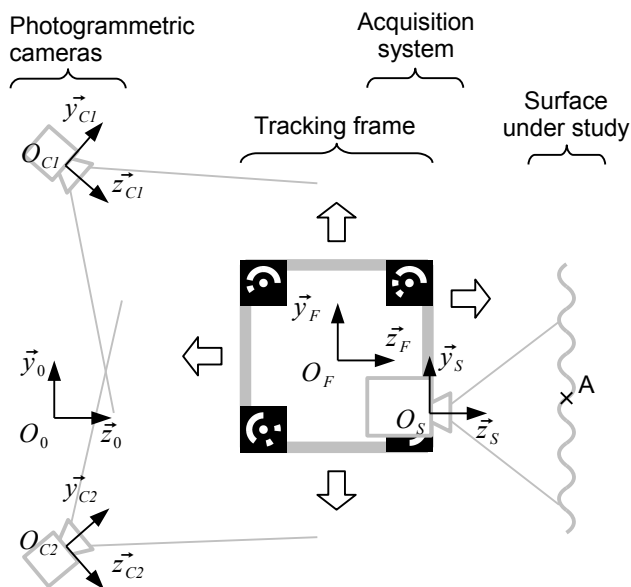


Figure 3: Coordinate systems defined for the tracking procedure.

78 *Internal orientation (I.O.) of the photogrammetric cameras.* The calibration of
 79 the tracking cameras is performed by taking close to a hundred images of a cal-
 80 ibration plate from various points of view. The calibration plate is covered with
 81 coded and uncoded targets and two distances are precisely known. From this
 82 we can measure the internal camera parameters such as focal length, principle
 83 point offset and lens distortion. The four tracking cameras are placed side by
 84 side and observe the same area so that they can be calibrated together. Previous
 85 experience has taught us that the internal orientation can stay stable for over
 86 a week if the cameras are handled with care during this time frame. We thus
 87 perform the interior orientation a few days before the acquisitions.

88 *Internal orientation of the acquisition system.* It is also necessary to know the
 89 distortions introduced by the acquisition system. In the case of the Atos III there
 90 is a specific calibration procedure to perform and the output data is corrected
 91 by the acquisition software.

92 *Calibration of the tracking frame.* The cube calibration is performed by taking
 93 over one hundred images of the tracking cube with a scale bar and additional
 94 targets. We can then define C_F and know the position of each coded target in
 95 this coordinate system.

96 *Orientation of the acquisition system with respect to the tracking frame.* To
 97 know the position of the acquisition system in the system defined by the tracking
 98 cube, we proceed in three steps:

- 99 1. Fix the acquisition system to the tracking frame.
 100 2. Use the acquisition system to digitize a target-covered 3D object.
 101 3. Take approximately fifty photos of the tracking frame and target 3D ob-
 102 ject.

103 We associate a coordinate system C_{temp} to the 3D object. Step 2 provides
 104 us with the position and orientation of the 3D object in C_S , that is $T_{S,temp}$.
 105 Similarly, step 3 provides us with the position and orientation of the 3D object
 106 in C_F previously defined, that is $T_{F,temp}$.

107 We can thus easily calculate the transformation between C_S and C_F : $T_{F,S} =$
 108 $T_{F,temp} \cdot (T_{S,temp})^{-1}$.

109 *Relative orientation of the photogrammetric cameras.* Once the tracking cam-
 110 eras have been positioned to observe the area in front of the surface under study,
 111 we can measure their relative position and orientation. This is done by acquiring
 112 approximately eighty images of a scalebar in various positions and orientations,
 113 simultaneously by the four calibrated cameras.

114 The position and orientation of the other three cameras are measured with
 115 respect to the first.

116 We choose the coordinate system of the first tracking camera as the world
 117 system: $C_0 = C_{C1}$.

118 2.4. Data processing

119 We thus have the necessary data to register the data sets. Each acquisition
 120 provides us with the coordinates of a group of surface points in the sensor system,
 121 $A|_{C_S}$. The simultaneous tracking provides us with T_{C_0,C_F} . The known interior
 122 orientation of the tracking cameras and their relative orientation ensures that
 123 T_{C_0,C_F} is sufficiently precise.

124 We can thus calculate $A|_{C_0}$, the coordinates of the surface points in the
 125 world system using:

$$A|_{C_0} = T_{C_0,C_F} \cdot T_{C_F,C_S} \cdot A|_{C_S} . \quad (1)$$

126 *Tracking and calibration software.* We rely on two pieces of software for all pho-
 127 togrammetric image processing: Tritop Deformation Software¹ and i3AxOri, a
 128 lab-developed software based on the AxOri photogrammetric bundle adjustment
 129 library². Tritop is used to recognize the coded and uncoded points in the im-
 130 ages and to compute a first assessment of the position of the cameras. This
 131 data is then exported to i3AxOri in which we have more flexibility and control
 132 on what we want to compute given our input parameters.

¹Gom, Tritop Deformation Software, <http://www.gom.com/3d-software/tritop-deformation-software.html>

²Axios 3D, Axori photogrammetric bundle block adjustment, <http://www.axios3d.de>

133 *Evaluating the registration accuracy.* The Gom Atos III acquisition software
 134 recognizes any coded or uncoded target present in the scene. In our case the
 135 full surface is covered with over 60 uncoded targets of diameter 6 mm. More
 136 than 10 targets are visible in each mesh. It is possible to export the list of the
 137 targets visible in each mesh. We thus have $A_{ij}|_{C_S}$ the coordinates of target
 138 point j from mesh i .

139 Using equation 1 we calculate $A_{ij}|_{C_0}$ for all targets of all meshes. For every
 140 target j we now calculate

$$D_{(i,k)_j} = A_{ij}|_{C_0} - A_{kj}|_{C_0} \quad (2)$$

141 for every pair of meshes (i, k) where target j is visible. If the registration
 142 were perfect, the result of this subtraction would be a null vector. Since the
 143 registration is imperfect, $D_{(i,k)_j}$ provides us a measure of the accuracy of the
 144 registration.

145 3. Results and Discussion

146 The various acquisitions were performed in the following order:

- 147 1. Photogrammetric cameras interior orientation (three days in advance)
- 148 2. Tracking frame calibration
- 149 3. Acquisition system interior orientation
- 150 4. Tracking frame to acquisition system orientation
- 151 5. Simultaneous digitization of the car door and photogrammetric tracking
 152 of the frame
- 153 6. Photogrammetric cameras exterior orientation

154 We first quickly present the accuracy achieved for the individual calibrations
 155 (steps 1 to 4 and 6). Then we analyze the accuracy with which we track the
 156 target frame (5) and finally we look in to the accuracy of the final registration.
 157 All accuracy values (simulations and measurements) are given at 2σ .

158 3.1. Individual calibrations

159 The accuracy of the individual calibrations described in section 2.3 is given
 160 in table 1. When available, they are compared with the expected accuracy
 161 of the simulations. The simulations were run with two levels of noise: low
 162 noise, corresponding to a best-case-scenario and higher noise, corresponding to
 163 a realistic situation. The accuracy reached is always in between the results for
 164 these two configurations.

165 The tracking cube calibration is performed with much higher accuracy than
 166 expected, though this value does not take into account the deformation that the
 167 aluminum cube may undergo due to temperature variations for example.

Table 1: Individual calibrations accuracy compared to expected accuracy from the simulations.

	Measures	Simulations		Unit
		realistic	best	
Photogrammetric cameras I.O.	0.055	0.1	0.033	pixel
Acquisitions system I.O.	0.020	***		pixel
Tracking frame calibration	0.015	0.05		mm
Tracking frame to acquisition system orientation	0.025	—		mm
	0.050	—		mrad
Photogrammetric cameras E.O.	0.017	0.03	0.01	mm
	0.030	0.02	0.04	mrad

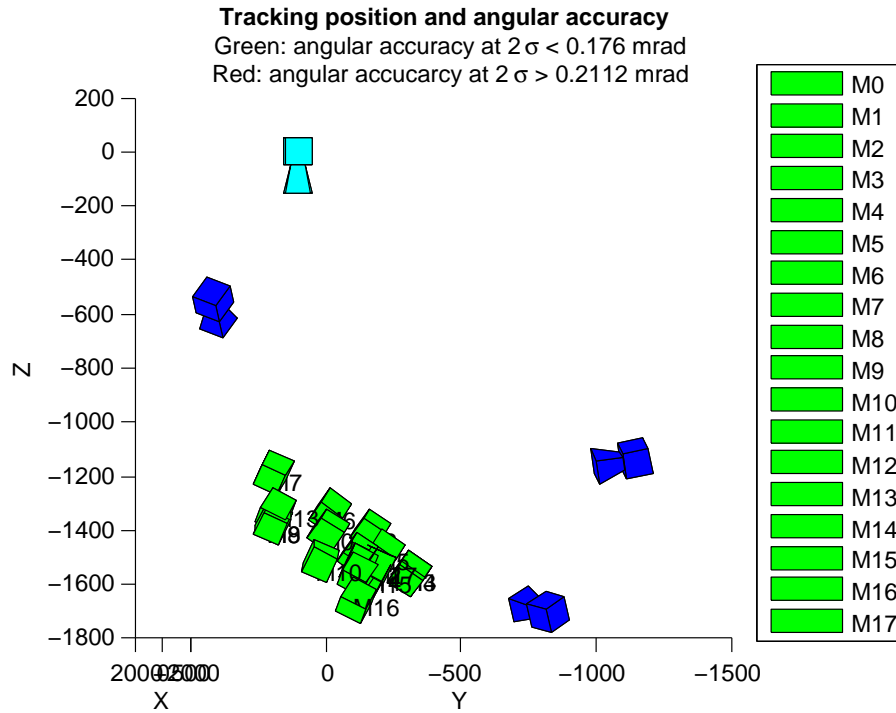


Figure 4: Relative position of the cameras (fixed, blue) and the tracking frame for all acquisitions. *** Redo: colors, orientation, remove text on figure and title

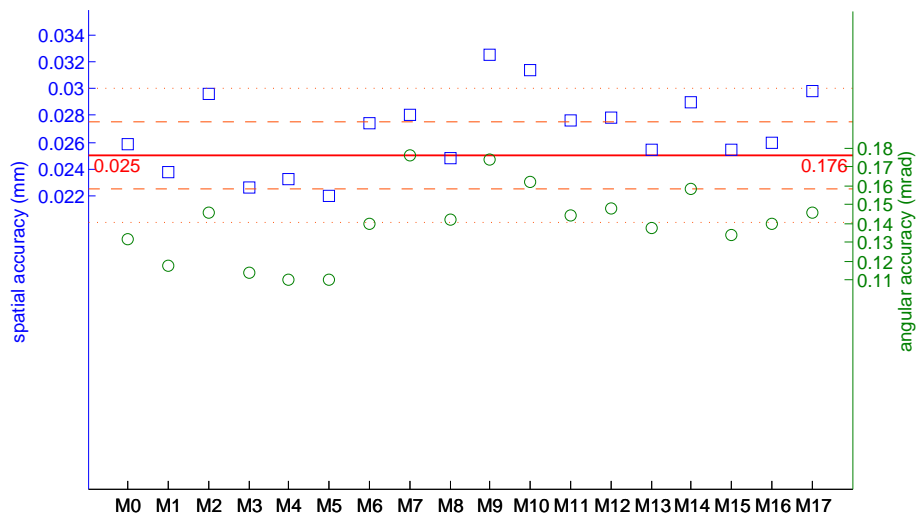


Figure 5: Spatial accuracy (blue squares) and angular accuracy (red circles) of the tracking for all 18 acquisition positions compared to the simulation results of the realistic scenario (red line).

168 *3.2. Tracking the frame*

169 Eighteen acquisitions are performed with the 3D digitization system. They
 170 are numbered M0 to M17. The relative position and orientation of the four
 171 tracking cameras and the tracking cube is illustrated figure 4.

172 This subsection examines the accuracy with which we evaluate T_{C_0, C_F} for
 173 each position. The spatial and angular accuracy achieved are compared to the
 174 simulation results of the realistic scenario figure 5. Though the spatial accuracy
 175 of the results is not as good as expected, the angular accuracy is always better
 176 than the value reached during the simulations.

177 Compared to the tracking accuracy target fixed by our registration goal
 178 (0.12 mm spatially and 0.158 mrad), the results are quite satisfying: the target
 179 spatial accuracy is always reached with a comfortable margin while the angular
 180 accuracy is insufficient for only three positions: M7, M9 and M10.

181 *3.3. Registration*

182 ***

183 **4. Conclusion and Perspectives**

- 184 • Contactless 3D acquisition and registration
- 185 • No need for targets
- 186 • Accuracy: ***

- 187 • Independent from sensor
- 188 • Different 3D sensors can be used
- 189 • Can be extended to 2D projection on 3D model
- 190 • Aluminum profiles are fine for rapid prototyping but they are heavy and
- 191 temperature dependent: a real object should be made of carbon

192 Acknowledgments

193 We would like to thank the Conseil Régional de Bourgogne, France , as well as
 194 i3mainz laboratory, Germany, for their funding and support. GOM lent us with
 195 a research license for Tritop which was greatly appreciated. Jens Bingenheimer
 196 helped perform the measurements. We thank him for his enthusiasm and his
 197 meticulousity.

198 References

- 199 [1] P. J. Besl, N. D. McKay, A Method for Registration of 3-D Shapes, IEEE
 200 Transactions on Pattern Analysis and Machine Intelligence 14 (1992) 239–
 201 256.
- 202 [2] S. Rusinkiewicz, M. Levoy, Efficient variants of the ICP algorithm, in:
 203 Proceedings of the Third International Conference on 3-D Digital Imaging
 204 and Modeling, Quebec City, Quebec, Canada, pp. 145–152.
- 205 [3] J. Hefele, Real-time photogrammetric algorithms for robot calibration, In-
 206 ternational Archives of Photogrammetry and Remote Sensing XXXIV (2002)
 207 33–38.
- 208 [4] T. Clarke, X. Wang, The control of a robot end-effector using photogramme-
 209 try, International Archives of Photogrammetry and Remote Sensing XXXIII
 210 (2000) 137–142.
- 211 [5] R. Schütze, C. Raab, F. Boochs, H. Wirth, J. Meier, Optopose - a multi-
 212 camera system for fast and precise determination of position and orientation
 213 for moving effector, in: 9th Conference on Optical 3D Measurement Tech-
 214 niques, Vienna, Austria.
- 215 [6] H.-G. Maas, Dynamic photogrammetric calibration of industrial robots, in:
 216 Proceedings of SPIE Vol 3174 Videometrics V, SPIE, San Diego, CA, USA,
 217 1997, pp. 106–112.
- 218 [7] C. Simon, R. Schütze, F. Boochs, F. S. Marzani, Asserting the Precise Posi-
 219 tion of 3D and Multispectral Acquisition Systems for Multisensor Registra-
 220 tion Applied to Cultural Heritage Analysis, in: K. Schoeffmann, B. Merialdo,
 221 A. G. Hauptmann, C.-W. Ngo, Y. Andreopoulos, C. Breiteneder (Eds.),
 222 MMM, volume LNCS 7131, Springer-Verlag Berlin Heidelberg, Klagenfurt
 223 (Austria), 2012, pp. 597–608.